Interferon-Stimulated Exonuclease Gene 20 is A Prognosis and Predictive Biomarker and Correlated with Macrophages M2 Polarization in Glioblastoma: A Pan-Cancer Analysis

Haiping Jiang
The First Affiliated Hospital of Harbin Medical University
Dongzhi Zhang
The First Affiliated Hospital of Harbin Medical University
Wenwu Liu
The First Affiliated Hospital of Harbin Medical University
Lixiang Wang
The First Affiliated Hospital of Harbin Medical University
Karpov Denis Aleksandrovich
The First Affiliated Hospital of Harbin Medical University
Xin Chen
The First Affiliated Hospital of Harbin Medical University
Cheng Zhang
Suffolk University
Jianing Wu
Shenzhen University General Hospital
Penglei Yao
Shenzhen University General Hospital
Zhenying Sun
Shenzhen University General Hospital
Xuan Rong
Shenzhen University General Hospital
Sokhatskii Andrei
The First Affiliated Hospital of Harbin Medical University
Xiaofeng Chen
The First Affiliated Hospital of Harbin Medical University
Shiguang Zhao (guangsz@hotmail.com)
The First Affiliated Hospital of Harbin Medical University

Research Article

Keywords: ISG20, isocitrate dehydrogenase 1 mutation, glioblastoma, macrophage M2

Posted Date: January 14th, 2022

DOI: https://doi.org/10.21203/rs.3.rs-1238023/v1

Abstract

Background: Since the mutation of isocitrate dehydrogenase 1 was confirmed to be different in the tumor microenvironment of multiple cancer types, several researchers have included it in the study of tumor-infiltrating immune cells. Interferon-stimulated exonuclease gene 20 (*ISG20*) plays a role in the modulation of immunity and inflammation, and its abnormally high expression is conducive for the progression of tumor malignancy. However, whether *ISG20* is associated with isocitrate dehydrogenase 1 mutation during tumorigenesis and cancer progression remains unknown to date.

Methods: TIMER2.0, ONCOMINE, GEPIA2, TCGA and CGGA were applied to assess the clinical significance of *ISG20* and its correlation with tumor-infiltrating immune cells in glioma. cBioPortal and MethSurv databases were used to observe the genetic and DNA methylation changes of *ISG20*, respectively. Visualization of data was mostly achieved by R language. Quantitative real-time PCR (qRT-PCR) and Immunohistochemistry (IHC) was performed to evaluate the mRNA and protein expression.

Results: *ISG20* expression was significantly different in most cancers. However, when we combined *ISG20* with isocitrate dehydrogenase 1 mutation, we found significant differences only in glioblastoma (GBM). The clinical values of *ISG20* in glioblastoma showed that the *ISG20* overexpression was strongly associated with a worse overall survival (OS). Additionally, *ISG20* was altered in 9% of samples of patients with GBM, and *ISG20* expression was negatively correlated with its DNA methylation level. More importantly, *ISG20* expression was associated with macrophage alternatively activated (M2) polarization in glioblastoma.

Conclusions: *ISG20* overexpression is conducive to malignant phenotype but adverse to OS, suggesting that *ISG20* is a potential therapeutic target and prognosis and predictive biomarker in patients with GBM.

1. Introduction

Complex and dynamically changing tumor microenvironments (TMEs) play a crucial role in sustained growth, differentiation, invasion, poor immunogenicity, and immunosuppression of cancer[1, 2]. Isocitrate dehydrogenase 1 (IDH1) is a nicotinamide adenine dinucleotide phosphate (NADP+)-dependent enzyme located in the cytoplasm, and its mutant form can convert α-ketoglutarate (α-KG) to the oncometabolite, 2-hydroxyglutarate (2-HG). 2-HG regulates cellular metabolism, redox states, and DNA repair, and induces genome-wide epigenetic changes, such as the glioma–CpG island methylator phenotype, which predisposes the cells in the TME to malignant transformation[3, 4]. As previously reported, IDH1 mutation (IDH1mut) in cancer often occurs at residue R132, which alters the catalytic activities of IDH1 and causes 2-HG accumulation. Thereby, histone methylation and gene expression are further changed, and this may contribute to the development of cancer[5, 6]. For example, (R)-2-HG can promote leukemogenesis, an effect that is reversible[7]. IDH1mut appears to first occur, followed by chromosome 1p/19q co-deletion or carriage of a tumor protein p53 gene (TP53) mutation, which promotes glioblastoma (GBM) to evade antitumor immune responses[8]. In addition, IDH1mut tumors,

compared to IDH1 wild type (IDH1wt) tumors, can reduce interferon (IFN)-γ-inducible cytokines in the tumors[9, 10].

It has been documented that several regulators such as extracellular vesicles, chemokines, growth factors and cytokines can contribute to the communication between cancer cells and the TME[11, 12]. IFNs are cytokines that activate the Janus kinase (JAK)-signal transducer and activator of transcription (STAT) pathway, which regulates the expression of many IFN-stimulated genes (ISGs)[13]. One such ISG, IFN-stimulated exonuclease gene 20 (*ISG20*), also known as HeLa estrogen-modulated, band 45 (HEM45), is a member of RNA exonuclease superfamily. Expression of *ISG20* is regulated by double-stranded RNA or IFN types I and II[14] and it is involved in tumorigenesis, progression, angiogenesis, and immune modulation[15, 16].

In the past, the central nervous system (CNS) is thought to be an immune-privileged organ, but recently it has been found that the CNS is only immunocompromised, but can still produce an immune response when diseases occur. Microglia and macrophages are critical tumor-associated immune cells and account for 20%–30% in some highly aggressive tumors[17]. As one of the most abundant tumor-infiltrating immune cells (TIICs) in the TME, macrophages play a key role in tumor pathogenesis and have two major polarization phenotypes (M1 and M2). M2 macrophages, contrary to the M1 cells that are pro-inflammatory and possess anti-tumor functions, are mainly involved in anti-inflammatory responses and promote tumor growth[18, 19].

However, whether the gene *ISG20* is correlated with IDH1 mutation and macrophage M2 polarization in aggressive tumors is unknown. In the present study, our results demonstrated that *ISG20* expression was significantly different in most cancers. However, when we combined *ISG20* with IDH1 mutation, we found significant differences only in GBM. Therefore, it is important to assess the correlation between *ISG20* and clinical prognosis factors and identify the potential molecular mechanisms in GBM. Additionally, we examined the correlation between *ISG20* and survival status, genetic alterations, DNA methylation, immune infiltration, and identified the relevant cellular pathways.

2. Materials And Methods

2.1. Data collection

Non-tumor brain tissues (n = 5), low-grade glioma (LGG; n = 7), and GBM (n =9) samples were collected from the First Affiliated Hospital of Harbin Medical University. This study was approved by the Clinical Research Ethics Committee of Harbin Medical University and was conducted in accordance with the Declaration of Helsinki. All the participants provided written informed consent. Transcriptome sequencing data of 325 glioma samples and 20 normal brain tissues and clinical data were downloaded from the Chinese Glioma Genome Atlas (CGGA) database. From the Cancer Genome Atlas (TCGA) database (https:// www.cbioportal.org/study/summary?id=GBM_ tcga) and public databases (https:// portal.gdc.cancer.gov/ and http: //www. cbioportal. org/), the following were downloaded: mRNA-seq data of 698 glioma samples and five normal brain tissues. Clinical data were also downloaded from a

public database (http: //www. cbioportal. org/). Data on *ISG20* methylation and its copy number alterations (CNAs) were also downloaded from TCGA database (http: //www. cbioportal. org/study/summary? id=GBM_tcga).

2.2. TIMER2.0, GEPIA2, and ONCOMINE analyses

The TIMER2.0 website (http://timer.cistrome.org/) was used to identify differences in *ISG20* expression between tumors and adjacent normal tissues for the different tumors. It was used to further analyze the expression of *ISG20* according to IDH1mut status. The GEPIA2 (Gene Expression Profiling Interactive Analysis, version 2) web server (http://gepia2.cancer-pku.cn/#analysis) and ONCOMINE database (http://www. oncomine.org) were used to verify the expression.

2.3. Genetic alteration analysis

First, we logged into the cBioPortal website (https://www.cbioportal.org/) and selected the Glioblastoma Multforme “TCGA Pan Cancer Atlas” under the mRNA expression z-score setting (RNA Seq V2 RSEM) with a z-score threshold of ±1.8. Next, we examined the mutation type, alteration frequency, and mutated site of the *ISG20* gene; then we analyzed the survival outcome of GBM patients with or without *ISG20* genetic alteration.

2.4. DNA methylation analysis

Using the MethSurv database (https://biit.cs.ut.ee/methsurv/) to screen the CpG island methylation sites of *ISG20* in GBM, we validated the relationship between the key methylation sites and overall survival (OS) time of GBM patients. DNA methylation data were obtained from TCGA Genome Data Analysis Center Firehose (http://gdac.broadin-stitute.org/) using the HM450K array. The methylation status of DNA is represented as β-values (0-1).

2.5. Functional correlation analysis

Pearson correlation analysis was performed to confirm the correlations between *ISG20* and other genes in whole-genome gene profiling of 169 GBM patients in the TCGA RNA-seq set. Significantly related genes ($|R| > 0.5$, $P < 0.05$) were mapped to Gene Ontology (GO) functional annotation and Kyoto Encyclopedia of Genes and Genomes (KEGG) pathways analyses using the “clusterProfiler” package in R language and Gene Set Variation Analysis (GSVA R package http://www.bioconductor.org/) was used to verify the relationship between *ISG20* and the candidate pathways.

2.6. Analysis of Immune Cell Characteristics

“CIBERSORT” (R package) was used to confirm the proportions of the 22 TIICs in each glioma patients’ sample. Moreover, we validated the correlation of *ISG20* expression with macrophages and tumor purity in GBM using the TIMER2.0 database.

2.7. Quantitative real-time polymerase chain reaction (qRT-PCR)

Total RNA was extracted from glioma samples using TRIzol reagent (Sigma, USA). cDNA synthesis was carried out using a ReverTra Ace qRT-PCR kit (Toyobo, Osaka, Japan). Quantitative RT-PCR was implemented on triplicate samples in a reaction mixture of SYBR Green (Roche, Basel, Switzerland) with a Gene Amp PCR System 9700 (Thermo Fisher Scientific, Waltham, MA, USA). The data were normalized by glyceraldehyde 3-phosphate dehydrogenase (GAPDH) using the ΔΔCt method. The primer sequences for GAPDH and *ISG20* were as follows: ISG20, F-5'TGGACTGCGAGATGGTGG3, R-5'GGGTTCTGTAATCGGTGAT3; GAPDH, F-5'CACCCACTCCTCCACCTTTGA3, R-5'ACCACCCTGTTGCTGTAGCCA3'.

2.8. Immunohistochemistry (IHC) for *ISG20* expression

For the IHC assay, the tumor tissues were immediately placed in 10% formalin for fixation, followed by dehydration, paraffin embedding, and sectioning. Next, the sections were immunostained with primary antibodies and an anti-mouse/rabbit secondary antibody. Anti-*ISG20* antibody (BIOGOT, BS72481) was used at a dilution of 1:100.

2.9. Statistical analysis

Differences between two groups and multiple groups were estimated using the Student's *t*-test and one-way analysis of variance, respectively. Pearson's correlation coefficients were used to analyze the relationships between variables, and the statistical significance of the prognostic value between different groups was evaluated using the log-rank test. All statistical analyses were performed using GraphPad Prism 7.0 and R 3.6.2. $P < 0.05$, was considered statistically significant. *, $P < 0.05$; **, $P < 0.01$; ***, $P < 0.001$; ****, $P < 0.0001$.

3. Results

3.1 Differential expression of *ISG20* in various tumors and in different IDH1mut states

Based on the TCGA dataset, we used the TIMER2.0 website to investigate *ISG20* mRNA expression in various cancer types and found that *ISG20* expression was significantly different when most tumors were compared with normal tissues. With breast invasive carcinoma (BRCA), cholangiocarcinoma (CHOL), esophageal carcinoma (ESCA), GBM, head and neck squamous cell carcinoma (HNSC), kidney renal clear cell carcinoma (KIRC), kidney renal papillary cell carcinoma (KIRP), liver hepatocellular carcinoma (LIHC), lung adenocarcinoma (LUAD), and uterine corpus endometrial carcinoma (UCEC), *ISG20* expression was significantly upregulated. *ISG20* expression was downregulated in colon adenocarcinoma (COAD), kidney chromophobe (KICH), lung squamous cell carcinoma (LUSC), rectum adenocarcinoma (READ), skin cutaneous melanoma (SKCM), and thyroid carcinoma (THCA). These results suggest that *ISG20* may have different regulatory mechanisms in different tumors (Fig. 1A). Next, by combining *ISG20* with IDH1mut, we found that there were significant differences only in GBM, lower grade glioma (LGG), and prostate adenocarcinoma (PRAD) (Fig. 1B-E, Table. S1). To further verify *ISG20* expression between normal samples and tumor tissues of GBM, LGG, and PRAD, we examined the GEPIA2 website and found

that the expression level of *ISG20* was statistically different only in GBM. These results indicate that *ISG20* could play crucial roles in the tumor progression of GBM.

3.2 Transcription levels of *ISG20* in GBM Patients

To verify *ISG20* mRNA expression between normal human brain tissues and GBM using ONCOMINE databases, our results showed that the transcription levels of *ISG20* were significantly elevated in patients with GBM in four datasets (Fig. 2A-E). Next, a meta-analysis of the mRNA expression levels of *ISG20* between GBM and non-tumor brain tissues was performed using the ONCOMINE database. *ISG20* mRNA expression was markedly upregulated in GBM tissues (*P*=1.31E-5) compared to those in non-tumor brain tissues, and the median rank of *ISG20* was 945.5 in GBM tissues (Fig. 2F).

3.3 *ISG20* expression was upregulated in GBM tissues and IDH1wt group, and its overexpression was unfavorable for the prognosis of GBM patients

LGG, GBM, and normal brain tissues with *ISG20* mRNA expression profiles and corresponding clinical information were obtained from the TCGA database. First, we found that *ISG20* mRNA expression in GBM tissues was upregulated compared to that in non-tumor and LGG tissues (Fig. 3A), but there was no difference between LGG tissues and non-tumor tissues. Moreover, low *ISG20* expression was more favorable for IDH1mutation (Fig. 3B). More importantly, our results revealed that high *ISG20* mRNA expression has a shorter OS time in patients with GBM (Fig. 3C). All the above results were verified using the CGGA data (Fig. 3D-F). Subsequently, we plotted the receiver operating characteristic curve (ROC) for *ISG20* mRNA expression and IDH1wt subtype of GBM to reconfirm the above finding. Interestingly, the areas under the curve (AUC) were 0.795 and 0.799 in the TCGA RNA-seq set and CGGA RNA-seq set, respectively (Fig. 3G, H). We also collected non-tumor human brain tissues and fresh glioma tissues to detect *ISG20* mRNA and protein expression using qRT-PCR (Fig. 3I) and IHC (Fig. 3J) analyses. The results demonstrated that *ISG20* mRNA and protein expression were both increased in GBM tissues compared to those in non-tumor human brain and LGG tissues. Moreover, IHC analysis showed that compared with the IDH1mut group, *ISG20* protein expression was higher in the IDH1wt group (Fig. 3K). Collectively, our results demonstrate that *ISG20* expression is upregulated in human IDH1wt GBM tissues, and high *ISG20* expression predicts a poor prognosis in GBM patients.

3.4 Genetic alteration of *ISG20* in GBM

Genetic and epigenetic changes play a crucial role in regulating cancer development and TIICs. First, we used cBioPortal to observe the genetic alteration status of *ISG20* in GBM and found that *ISG20* was altered in 14/155 (9%) GBM patient samples (Fig. 4A). The types of genetic alterations included mutation, amplification, and high and low mRNA levels. Simultaneously, we found that *ISG20* had one missense mutation, R27C, in its RNase-T domain (Fig. 4B), and observed the R27C site in the 3D structure of *ISG20* protein (Fig. 4C). Additionally, we found that compared with the unaltered group, the altered group of *ISG20* had favorable OS, disease-free survival (DFS), and progression-free survival (PFS) in GBM patients (Fig. 4D, E, and F). Furthermore, we explored somatic mutations between cases with low and high *ISG20*

mRNA expressions and found that mutations in TP53, epidermal growth factor receptor (EGFR), and SPTA1 were significantly enriched in low *ISG20* mRNA expression cases (Fig. 4G). However, gliomas with high ISG20 mRNA expression possessed higher frequency of PTEN and TTN mutations (Fig. 4G). Subsequently, we also explored CNAs in glioma according to *ISG20* mRNA expression, and observed that chromosome (Chr) 7 was significantly amplified in gliomas, on the contrary, Chr 10 was deleted (Fig. 4H); simultaneously, 7p11.2 and 15q24.3 peaks were significantly amplified in gliomas with high *ISG20* mRNA expression (Fig. 4I). Thus, the anomalous increase of *ISG20* mRNA expression in GBM is likely caused by genetic alterations. Next, we demonstrated whether epigenetic mechanisms are involved in the regulation of *ISG20* mRNA expression.

3.5 *ISG20* DNA methylation and their prognostic values in GBM

DNA methylation is an epigenetic form of regulating gene expression without altering the sequence of the genome[20]. First, we performed the Pearson correlation analysis to investigate the correlation between *ISG20* mRNA expression and its DNA methylation levels in GBM and found a significantly negative correlation between them (Fig. 5A). Subsequently, the β values of all eleven *ISG20* CpG sites in GBM according to HM450K arrays were analyzed and displayed using MethSurv tool (Fig. 5B). Among them, the CpG sites cg19951424 (1stExon; 5'UTR), cg24181188 (1stExon; 5'UTR), and cg04515913 (1stExon; 5'UTR) showed low DNA methylation levels. In addition, clustering analysis in the form of heat maps showed that methylation sites cg1995142, cg24181188, and cg04515913 in the '1stExon; 5'UTR' sub-region had differential hypo-methylation levels in GBM patients (139 samples) (Fig. 5C), which was consistent with the β values presented in Fig. 5B. Furthermore, to evaluate the prognostic value of each CpG site, our results revealed that only the DNA methylation levels of cg24181188 were negatively correlated with OS in GBM patients, using the median of DNA methylation level (Fig. 5D, Fig. S1A, B). Finally, we observe that the methylation level of cg24181188 (R2 = 0.1337) was also decreased, accompanied by an increase in *ISG20* expression ($P < 0.05$) (Fig. 5C). Thus, these findings demonstrated that increased *ISG20* mRNA expression in GBM samples could be associated with hypomethylated CpG sites.

3.6 Functional enrichment analysis of *ISG20* in patients with GBM

To investigate the biological processes of *ISG20* in GBM, Pearson correlation analysis between ISG20 and other genes was performed using the TCGA RNA-seq set. We then chose 301 genes that were most relevant to *ISG20*($|R| > 0.5$, $P < 0.05$) to draw the heat maps (Fig. 6A) and performed enriched GO and KEGG analyses. GO results showed that the major biological processes included response to IFN-γ, neutrophil activation involved in immune response, neutrophil activation and degranulation, antigen processing and presentation, response to tumor necrosis factor, and response to virus (Fig. 6B). The major cellular components (CCs) were collagen-containing extracellular matrix, secretory granule lumen, vesicle lumen, focal adhesion, major histocompatibility complex protein, and lysosomes (Fig. 6C). The major molecular functions (MFs) were enzyme inhibitor activity, protease binding, peptide antigen binding, 1 phosphatidylinositol 3 kinase regulator activity, immunoglobulin binding, and cysteine-type

endopeptidase activity involved in the apoptotic process (Fig. 6D). KEGG pathway analysis revealed that *ISG20* is mainly involved in *Salmonella* infection, HIV 1 infection, phagosomes, antigen processing and presentation, natural killer cell-mediated cytotoxicity, and complement and coagulation cascades (Fig. 6E). We also performed gene set enrichment analysis (GSEA) between *ISG20* expression and other genes in the TCGA database. The GSEA data showed that allograft rejection, inflammatory response, E2F targets, G2M checkpoint, mammalian Target of rapamycin complex 1 (mTORC1) signaling, hypoxia, mitotic spindle, p53, and KRAS signaling up, and early estrogen response were enriched in the high *ISG20* mRNA expression group (Fig. 6F). Therefore, our results indicate that *ISG20* is involved in immune regulation in glioma, and we next explored its relationship with TIICs.

3.7 *ISG20* expression is correlated with immune infiltration levels and macrophages M2 polarization in glioma patients

TIICs, as crucial components of the TME, induced consequences for the initiation, progression, and outcome of cancer[21, 22]. Therefore, we studied the potential immunological correlation between *ISG20* and TIICs. First, we used the CIBERSORT algorithm to determine the levels of the 22 types of immune cells (Fig. 7A, B). Macrophages M2 and CD4 memory resting T cells accounted for a large proportion of glioma infiltrating immune cells, consistent with previous studies[17]. By comparing the high *ISG20* and low *ISG20* expression groups; LGG and GBM groups; and IDH1wt and IDH1mut groups, we found significant differences in the infiltrated levels of macrophage M2 between them but not in the immune cell abundance of CD4 memory resting T cells (Fig. 7C, Fig. S2A, B). Subsequently, we used TIMER2.0 database to explore the relationship of *ISG20* mRNA expression with tumor purity and macrophage M2 in GBM, and found that *ISG20* mRNA expression was negatively correlated with tumor purity ($P < 0.05$) (Figure 7E), indirectly indicating that high *ISG20* mRNA expression may predict an unfavorable prognosis, since previous studies showed that tumor purity reflects the characteristics of TME and low tumor purity is associated with poor outcome of glioma[23]. Simultaneously, our results further verified that *ISG20* mRNA expression was positively correlated with M2 macrophage infiltration levels (Fig. 7F-H). Finally, we analyzed the correlation between macrophage M2 markers and *ISG20* expression, and the grade of glioma and IDH1 mutation status to explore the possible molecular mechanism of macrophage M2 polarization. Our results showed that the expression of CD163 and CD204 were all up-regulated in high *ISG20* expression, GBM, and IDH1wt groups compared to low *ISG20* expression, LGG, and IDH1mut groups, respectively (Fig. 7D, Fig. S2C, D). On the contrary, CD206, another marker of M2 macrophages, was decreased in high *ISG20* expression and IDH1wt groups compared to low *ISG20* expression and IDH1mut groups, and not different between LGG and GBM groups (Fig. 7D, Fig. S2C, D). These further demonstrate that macrophage M2 polarization is regulated by multiple molecular mechanisms. Moreover, IHC was performed; our results revealed that compared to the LGG and low *ISG20* groups, the protein expression of CD163 and CD204 were higher in GBM and high *ISG20* expression groups (Fig. 7I, J); however, CD163 and CD204 protein expression was lower in the IDH1mut group than in the IDH1wt group (Fig. 7K). Collectively, our data demonstrated that *ISG20* high expression was correlated with macrophages M2 cells infiltration levels in GBM. The high expressions of CD163 and CD204 are likely the

results of *ISG20* high expression, and macrophages M2 polarization predicted malignant biological phenotypes in glioma.

4. Discussion

Cytokines are low molecular weight soluble proteins released by cancer cells or stromal cells and required for the formation of TME, because cytokines can regulate innate and adaptive immunity, hematopoiesis, cell growth, and repair of damaged tissues through endocrine, autocrine, and paracrine modes, and enable cells in TME to communicate[24, 25]. IFNs are cytokines that modulate resistance to viral infections, inhibit cell proliferation, adjust immunity and anti-tumor effects, and induce the production of hundreds of ISGs[26, 27]. *ISG20*, a human cDNA encoding promyelocytic leukemia nuclear bodies (PML-NBs)-associated protein[28], is an ISG that is directly induced by IFN[29]. It has been reported that promyelocytic leukemia (PML) is a tumor suppressor and essential for the proper assembly of PML-NB (which contains over 70 proteins) and its anti-tumor functions, according to its binding protein[30-33]. In addition, *ISG20* expression has been shown to be up-regulated during infection and in several types of cancers, including glioma[16, 34-38]. In these cancers, *ISG20* high expression indicates a poor OS. However, systematic and comprehensive analyses to further elucidate *ISG20* underlying role in tumors are lacking. In the current study, our results revealed that *ISG20* was highly expressed in most cancers using a pan-cancer analysis.

In addition, IDH1 is an NADP+-dependent enzyme located in the cytoplasm, and its mutant form can convert α-KG to the oncometabolite 2-HG[3]. The enrichment of 2-HG produced by IDH1mut at residue R132 may be conducive to cancer development by inhibiting histone demethylases and collagen maturation, and upregulating HIF1α, leading to increased histone methylation and altered gene expression[39, 40]. To further explore the correlation between *ISG20* expression and IDH1mut status in different tumors, we combined *ISG20* with IDH1 mutation and found that there were significant differences only in GBM. In addition, our results showed that *ISG20* high expression seems to be linked to malignant entities, such as GBM and IDH1wt status in gliomas. Simultaneously, the OS curve indicated that *ISG20* high expression was detrimental to the survival of patients with GBM. To further explain this finding, ROC for *ISG20* expression and IDH1wt subtype of GBM were generated, and the AUC were 0.795 and 0.799 in the TCGA RNA-seq set and CGGA RNA-seq set, respectively. More importantly, we also collected non-tumor brain tissues and fresh glioma tissues to verify *ISG20* mRNA and protein expression and found that the expression of *ISG20* was higher in GBM and in its IDH1wt status compared to that in non-tumor tissues, LGG tissues and IDH1mut status, respectively. Summarily, our results indicate that *ISG20* expression is upregulated in human GBM tissues and its IDH1wt status, and high *ISG20* expression predict a poor prognosis in GBM patients.

Subsequently, we analyzed the possible mechanisms of *ISG20* high expression from genetic and epigenetic changes. First, we observed that *ISG20* was altered in 14/155 (9%) GBM patient samples and found that its alterations were conducive to OS, DSS, and PFS; simultaneously, our results revealed that the frequency of PTEN and TTN mutations increased in gliomas with high *ISG20* mRNA expression, and

the 7p11.2 and 15q24.3 peaks were significantly amplified. Thus, the abnormal increase of *ISG20* mRNA expression in GBM may be caused by genetic change and affect genomic alterations. Additionally, DNA hypomethylation is common in cancer and often leads to upregulation of oncogenes[41, 42]. Comparing *ISG20* mRNA expression with its DNA methylation level, we confirmed that *ISG20* mRNA expression was significantly inversely correlation with its DNA methylation level, indicating that methylation alteration may be another mechanism for the increase of *ISG20* mRNA expression. Because not all methylation sites are responsible for gene expression, the most significant methylation sites required further investigation. Eleven CpG sites were grouped into the *ISG20* gene sub-regions. Among them, cg19951424, cg24181188, and cg04515913 showed a low DNA methylation level, and their prognostic value in CpG site was explored. The results indicated that only DNA methylation levels of cg24181188 were statistically correlated with the prognosis of GBM patients.
Simultaneously, the methylation level of cg24181188 (R2 = 0.1337) also decreased, accompanied by an increase in the expression levels of *ISG20* ($P < 0.05$), which indicated that the change of cg24181188 may be one of the crucial epigenetic mechanisms for the increase of *ISG20* mRNA expression.

Regarding the biological functions of *ISG20*, we revealed that *ISG20* played a crucial role in the inflammatory response and immune regulation in GBM. To further investigate the association of *ISG20* expression with TIICs in glioma, we explored the abundance of TIICs, which are related to tumor progression, metastasis, or prognosis[21, 22]. The results showed that macrophages M2 and CD4 memory resting T cells accounted for a large proportion of glioma infiltration immune cells, and *ISG20* high expression contributed to macrophages M2 infiltration and was negatively correlated with GBM purity (percentage of malignant cells in a tumor tissue). However, *ISG20* expression exhibited no statistical correlation with the abundance of CD4 memory resting T cells in gliomas. In the TME, tumor-associated macrophages (TAMs) are considered to be of the polarized M2 phenotype, which enhances tumor progression and indicates a poor prognosis[43]. Therefore, we focused on the correlation between *ISG20* expression and markers of macrophages M2. These findings revealed that the expression of CD163 and CD204 were all up-regulated in high *ISG20* expression, GBM, and IDH1wt groups compared to low *ISG20* expression, LGG, and IDH1mut groups, respectively. However, CD206 was not different between LGG and GBM, and was negatively correlated with the high *ISG20* and IDH1mut groups, which can be explained by the fact that macrophage polarization is a complex process regulated by many factors. In the current study, we did not thoroughly explore the mechanism of CD206 abnormal expression, which will be verified in future studies. Therefore, our results showed that the polarization of macrophages M2 predicted malignant biological phenotypes in glioma and was likely the result of the abnormal high expression of *ISG20*.

Conclusion

In summary, our study is the first to evaluate *ISG20* combined with IDH1mut in tumors, by pan-cancer analysis. This study provides comprehensive evidence for *ISG20* as a potential therapeutic target and prognosis and predictive biomarker for GBM. However, the exact mechanisms by which *ISG20* regulates macrophage M2 polarization are largely unknown and need to be explored in future studies.

Abbreviations

ISG20: Interferon-stimulated exonuclease gene 20; IDH1: Isocitrate dehydrogenase 1; LGG: low-grade glioma; GBM: glioblastoma; qRT-PCR: quantitative real-time PCR; IHC: immunohistochemistry; OS: overall survival; TMEs: tumor microenvironments; TIICs: tumor-infiltrating immune cells; CNS: central nervous system; TCGA: the Cancer Genome Atlas; GO: Gene Ontology; KEGG: Kyoto Encyclopedia of Genes and Genomes; GSVA: Gene Set Variation Analysis; ROC: receiver operating characteristic curve.

Declarations

Acknowledgments

We would like to thank Editage (www. editage.cn) for English language editing and all reviewers and editors for their valuable comments on this study.

Funding

This work was funded by the Natural Science Foundation of China grants (81972363), and Heilongjiang Province Postdoctoral Fund (LBH-Z19076).

Availability of data and materials

Please contact author for data requests

Authors' contributions

HJ designed, conceived, planned, implemented the experiment, and wrote the original draft. LW and LW assisted in collecting clinical samples. DZ assisted in completing experiments. KA, XC, CZ, JW, PY, ZS, XR and SA participated in the investigation. XC and SZ supervised and funded the research. All authors read and approved the final manuscript.

Ethics approval and consent to participate

This study was approved by the Clinical Research Ethics Committee of Harbin Medical University and was conducted in accordance with the Declaration of Helsinki. All the participants provided written informed consent.

Consent for publication

Not applicable.

Competing interests

The authors declare no competing interests.

References

1. Dapash, M., et al., The Interplay between Glioblastoma and Its Microenvironment. *Cells*, 2021. **10**(9).
2. Hanahan, D. and L.M. Coussens, Accessories to the crime: functions of cells recruited to the tumor microenvironment. *Cancer Cell*, 2012. **21**(3): p. 309-22.
3. Dang, L., et al., Cancer-associated IDH1 mutations produce 2-hydroxyglutarate. *Nature*, 2009. **462**(7274): p. 739-44.
4. July, J., et al., Clinicopathological associations and prognostic values of IDH1 gene mutation, MGMT gene promoter methylation, and PD-L1 expressions in high-grade glioma treated with standard treatment. *Pan Afr Med J*, 2020. **36**: p. 309.
5. Bogdanovic, E., IDH1, lipid metabolism and cancer: Shedding new light on old ideas. *Biochim Biophys Acta*, 2015. **1850**(9): p. 1781-5.
6. Ye, D., K.L. Guan, and Y. Xiong, Metabolism, Activity, and Targeting of D- and L-2-Hydroxyglutarates. *Trends Cancer*, 2018. **4**(2): p. 151-165.
7. Issa, G.C. and C.D. DiNardo, Acute myeloid leukemia with IDH1 and IDH2 mutations: 2021 treatment algorithm. *Blood Cancer J*, 2021. **11**(6): p. 107.
8. Kristensen, B.W., et al., Molecular pathology of tumors of the central nervous system. *Ann Oncol*, 2019. **30**(8): p. 1265-1278.
9. Kohanbash, G., et al., Isocitrate dehydrogenase mutations suppress STAT1 and CD8+ T cell accumulation in gliomas. *J Clin Invest*, 2017. **127**(4): p. 1425-1437.
10. Gao, M., et al., ISG20 promotes local tumor immunity and contributes to poor survival in human glioma. *Oncoimmunology*, 2019. **8**(2): p. e1534038.
11. Han, L., E.W. Lam, and Y. Sun, Extracellular vesicles in the tumor microenvironment: old stories, but new tales. *Mol Cancer*, 2019. **18**(1): p. 59.
12. Li, L., et al., Effects of immune cells and cytokines on inflammation and immunosuppression in the tumor microenvironment. *Int Immunopharmacol*, 2020. **88**: p. 106939.
13. Place, D.E., et al., Osteoclast fusion and bone loss are restricted by interferon inducible guanylate binding proteins. *Nat Commun*, 2021. **12**(1): p. 496.
14. Van Tong, H., et al., Interferon-stimulated gene 20 kDa protein serum levels and clinical outcome of hepatitis B virus-related liver diseases. *Oncotarget*, 2018. **9**(45): p. 27858-27871.
15. Xu, T., et al., ISG20 serves as a potential biomarker and drives tumor progression in clear cell renal cell carcinoma. *Aging (Albany NY)*, 2020. **12**(2): p. 1808-1827.
16. Taylor, K.L., et al., Identification of interferon-beta-stimulated genes that inhibit angiogenesis in vitro. *J Interferon Cytokine Res*, 2008. **28**(12): p. 733-40.
17. Kong, L.Y., et al., Intratumoral mediated immunosuppression is prognostic in genetically engineered murine models of glioma and correlates to immunotherapeutic responses. *Clin Cancer Res*, 2010. **16**(23): p. 5722-33.

18. Williams, C.B., E.S. Yeh, and A.C. Soloff, Tumor-associated macrophages: unwitting accomplices in breast cancer malignancy. NPJ *Breast Cancer*, 2016. **2**.
19. Sica, A., et al., Tumour-associated macrophages are a distinct M2 polarised population promoting tumour progression: potential targets of anti-cancer therapy. *Eur J Cancer*, 2006. **42**(6): p. 717-27.
20. Li, B., et al., Expression signature, prognosis value, and immune characteristics of Siglec-15 identified by pan-cancer analysis. *Oncoimmunology*, 2020. **9**(1): p. 1807291.
21. Chen, T.H., et al., Tumor-infiltrating lymphocytes predict prognosis of breast cancer patients treated with anti-Her-2 therapy. *Oncotarget*, 2017. **8**(3): p. 5219-5232.
22. Almangush, A., et al., Tumor-infiltrating lymphocytes associate with outcome in nonendemic nasopharyngeal carcinoma: a multicenter study. *Hum Pathol*, 2018. **81**: p. 211-219.
23. Gong, Z., J. Zhang, and W. Guo, Tumor purity as a prognosis and immunotherapy relevant feature in gastric cancer. *Cancer Med*, 2020. **9**(23): p. 9052-9063.
24. Dougan, M., et al., Targeting Cytokine Therapy to the Pancreatic Tumor Microenvironment Using PD-L1-Specific VHHs. *Cancer Immunol Res*, 2018. **6**(4): p. 389-401.
25. Galdiero, M.R., G. Marone, and A. Mantovani, Cancer Inflammation and Cytokines. *Cold Spring Harb Perspect Biol*, 2018. **10**(8).
26. Stark, G.R. and J.E. Darnell, Jr., The JAK-STAT pathway at twenty. *Immunity*, 2012. **36**(4): p. 503-14.
27. Trinchieri, G., Type I interferon: friend or foe? J Exp Med, 2010. **207**(10): p. 2053-63.
28. Gongora, C., et al., A unique ISRE, in the TATA-less human Isg20 promoter, confers IRF-1-mediated responsiveness to both interferon type I and type II. *Nucleic Acids Res*, 2000. **28**(12): p. 2333-41.
29. Der, S.D., et al., Identification of genes differentially regulated by interferon alpha, beta, or gamma using oligonucleotide arrays. *Proc Natl Acad Sci U S A*, 1998. **95**(26): p. 15623-8.
30. Boisvert, F.M., M.J. Hendzel, and D.P. Bazett-Jones, Promyelocytic leukemia (PML) nuclear bodies are protein structures that do not accumulate RNA. *J Cell Biol*, 2000. **148**(2): p. 283-92.
31. Ching, R.W., et al., PML bodies: a meeting place for genomic loci? *J Cell Sci*, 2005. **118**(Pt 5): p. 847-54.
32. Block, G.J., et al., Transcriptional regulation is affected by subnuclear targeting of reporter plasmids to PML nuclear bodies. *Mol Cell Biol*, 2006. **26**(23): p. 8814-25.
33. Shen, T.H., et al., The mechanisms of PML-nuclear body formation. *Mol Cell*, 2006. **24**(3): p. 331-9.
34. Feng, H.H., et al., Foot-and-mouth disease virus induces lysosomal degradation of NME1 to impair p53-regulated interferon-inducible antiviral genes expression. *Cell Death Dis*, 2018. **9**(9): p. 885.
35. Lin, S.L., et al., Stimulation of Interferon-Stimulated Gene 20 by Thyroid Hormone Enhances Angiogenesis in Liver Cancer. *Neoplasia*, 2018. **20**(1): p. 57-68.
36. Miyashita, H., et al., ISG20 is overexpressed in clinically relevant radioresistant oral cancer cells. *Int J Clin Exp Pathol*, 2020. **13**(7): p. 1633-1639.
37. Rajkumar, T., et al., Identification and validation of genes involved in cervical tumourigenesis. *BMC Cancer*, 2011. **11**: p. 80.

38. Wang, J., et al., Development and validation of a hypoxia-related prognostic signature for breast cancer. *Oncol Lett*, 2020. **20**(2): p. 1906-1914.
39. Sasaki, M., et al., IDH1(R132H) mutation increases murine haematopoietic progenitors and alters epigenetics. *Nature*, 2012. **488**(7413): p. 656-9.
40. Lu, J., et al., IDH1 mutation promotes proliferation and migration of glioma cells via EMT induction. *J BUON*, 2019. **24**(6): p. 2458-2464.
41. Van Tongelen, A., A. Loriot, and C. De Smet, Oncogenic roles of DNA hypomethylation through the activation of cancer-germline genes. *Cancer Lett*, 2017. **396**: p. 130-137.
42. Ehrlich, M. and M. Lacey, DNA hypomethylation and hemimethylation in cancer. *Adv Exp Med Biol*, 2013. **754**: p. 31-56.
43. Mantovani, A., et al., Macrophage polarization: tumor-associated macrophages as a paradigm for polarized M2 mononuclear phagocytes. *Trends Immunol*, 2002. **23**(11): p. 549-55.

Figures

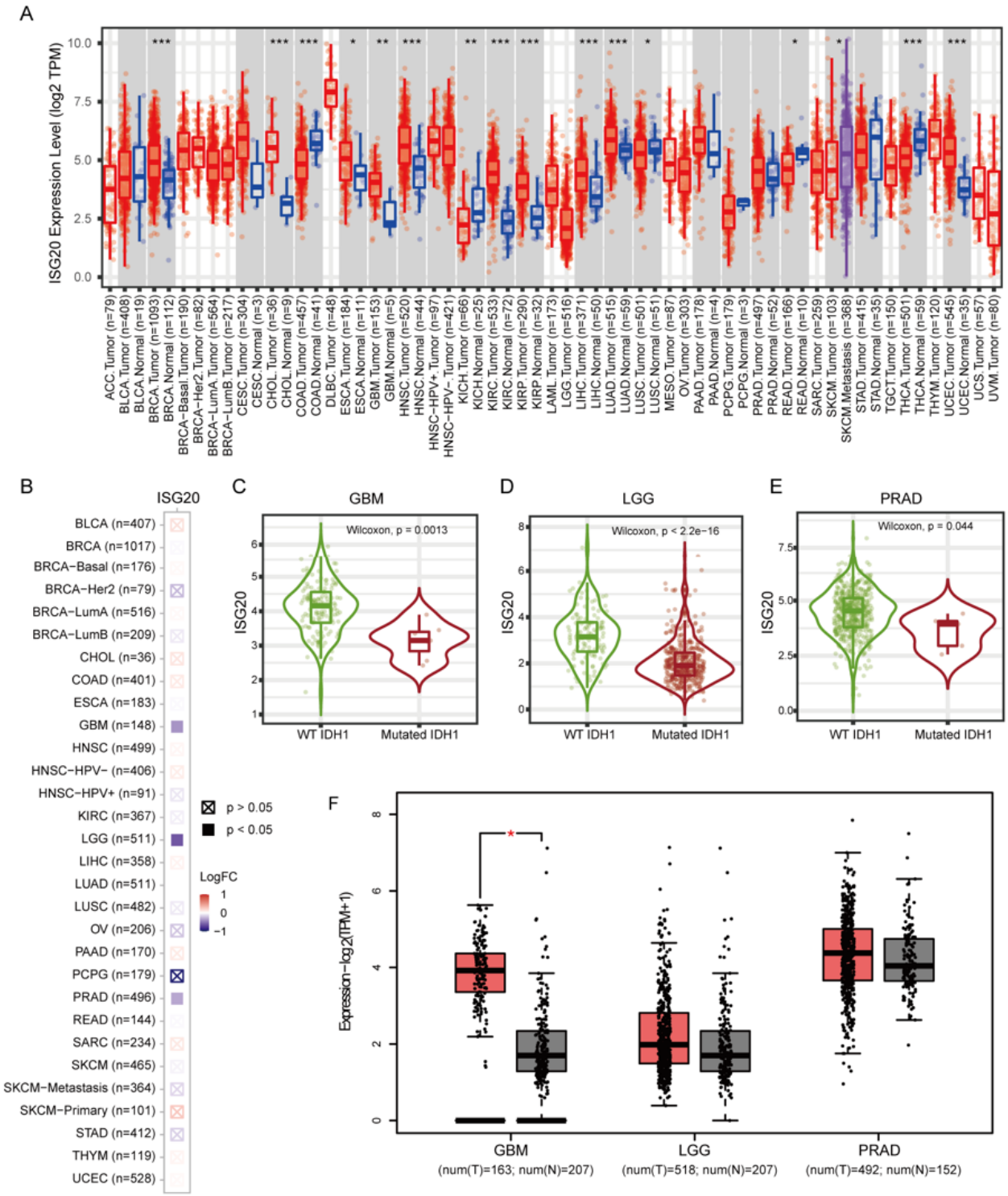

Figure 1

Differential expression of *ISG20* in various tumors and in different IDH1 mutation status. (A) The expression status of the *ISG20* gene in different cancers or specific cancer subtypes from TCGA database were analyzed by TIMER2. (B) The correlation between the expression level of *ISG20* and the IDH1 mutation status across all types of cancer in TCGA. (C-E) The correlation between the *ISG20* mRNA expression and IDH1 mutation status in GBM, LGG and PRAD was analyzed through TIMER2. (F) For the

type of GBM, LGG and PRAD in the TCGA project, the corresponding normal tissues of the GTEx database were included as controls. Box plots derived from gene expression data for GEPIA2 were supplied. *P*<0.05; * *P*<0.05; ** *P*<0.01; *** *P*<0.001.

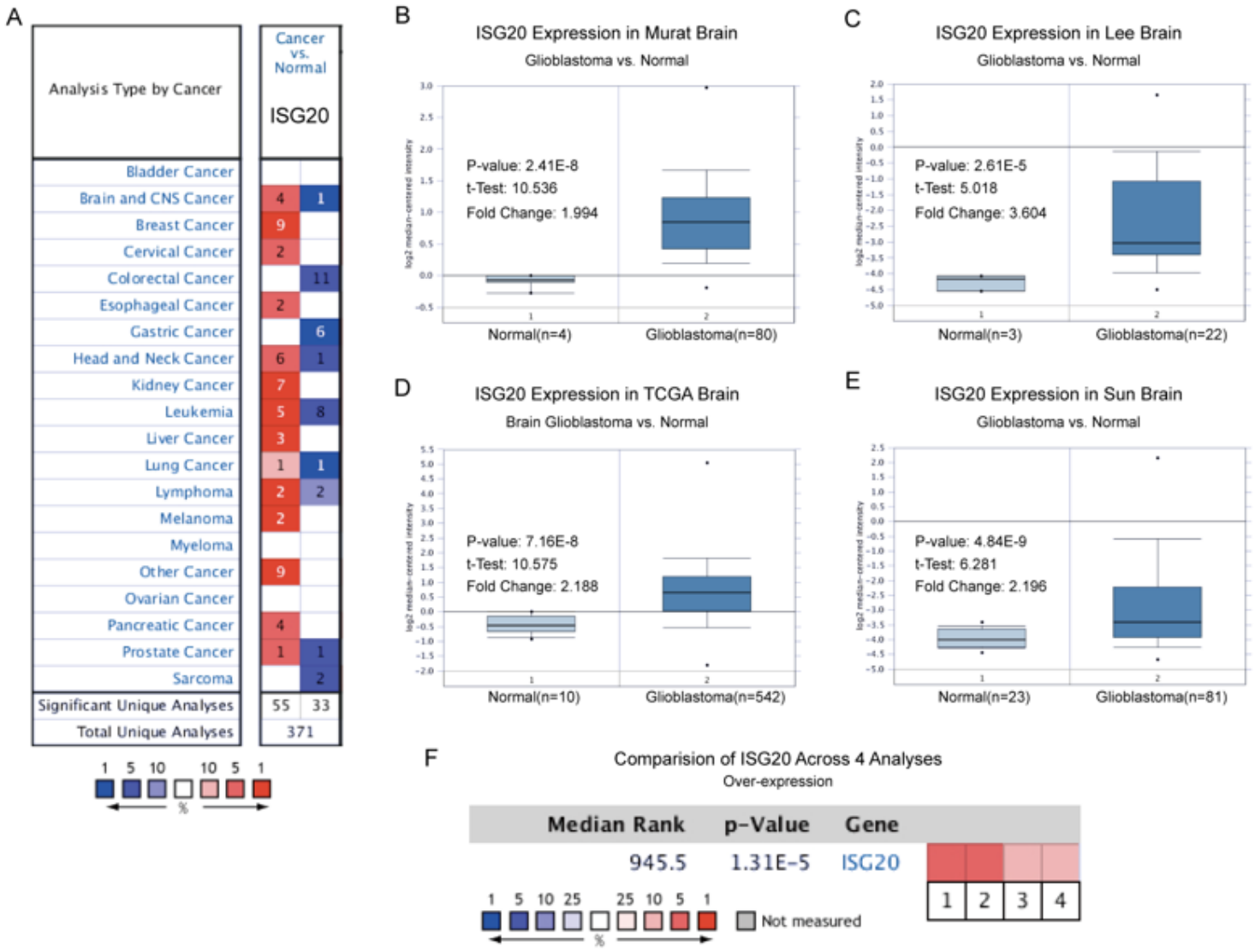

Figure 2

Transcription levels of *ISG20* in GBM Patients. (A) The heatmap represents data with statistically significant upregulation (red) or downregulation (blue) of *ISG20* transcription levels in various human cancer tissues as compared with their normal control. The numbers in the heatmap indicate the published independent datasets of mRNA microarray experiments. (B-E) Box plots from gene expression data in TCGA database comparing the expression of *ISG20* in normal and GBM tissue. (F) Meta-analysis on the mRNA expression levels of *ISG20* in GBM tissues vs. non-cancerous brain tissues using the four ONCOMINE datasets. The colored squares represent the median rank of these genes (vs. normal tissue) across the four datasets. The significance level for the median rank analysis was set at *P*<0.05.

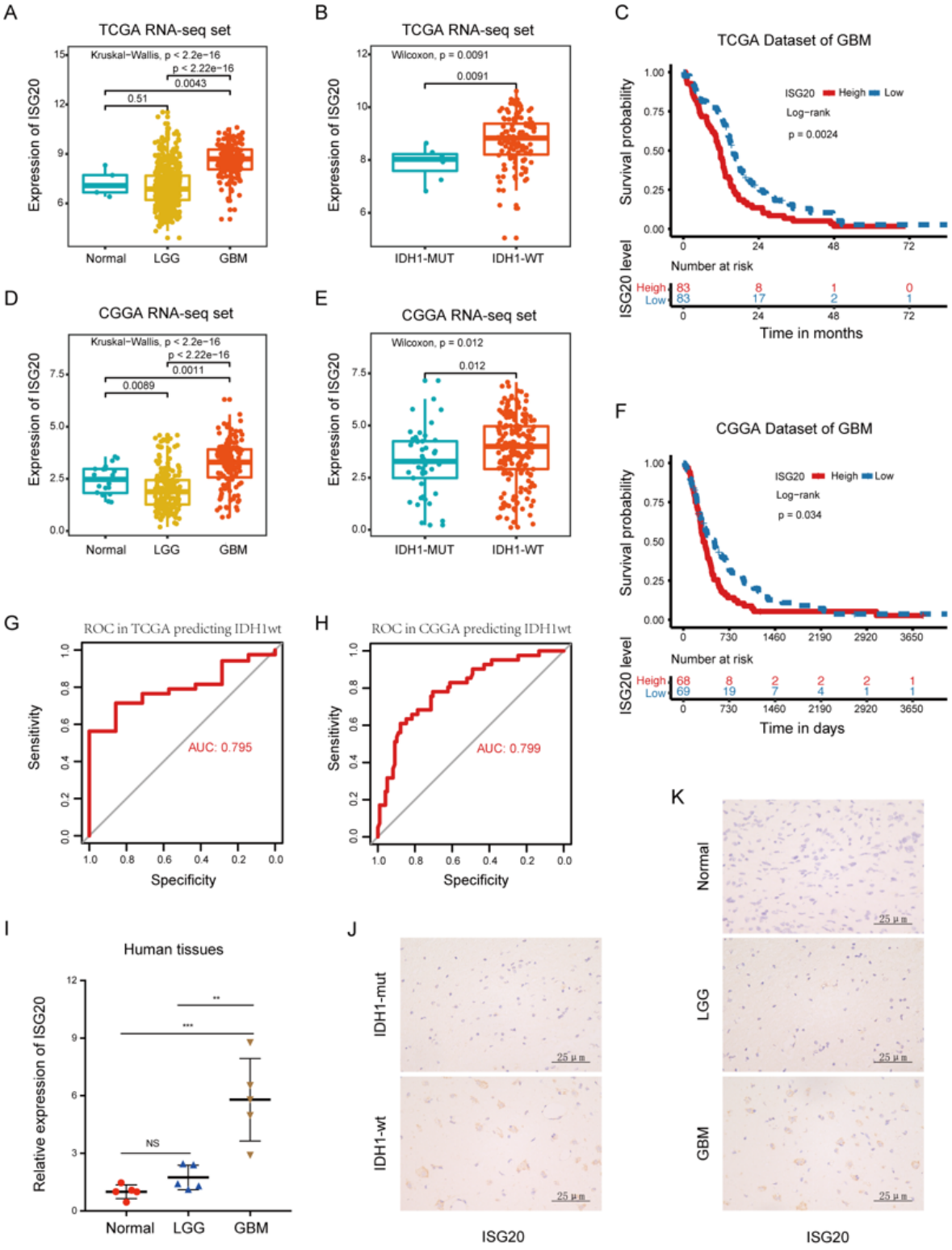

Figure 3

ISG20 expression was upregulated in human GBM tissues and IDH1wt group, and its overexpression was unfavorable for the prognosis of GBM patients. (A, D) Differential expression of *ISG20* mRNA in normal brain tissues, LGG tissues and GBM tissues in TCGA and CGGA, respectively. (B, E) The correlation between the *ISG20* mRNA expression and IDH1 mutation status in GBM were analyzed by TCGA database and CGGA database, respectively. Kaplan-Meier survival analysis of *ISG20* in GBM based on the

TCGA cohort (C) and CGGA cohort (F). ROC curves of *ISG20* expression to predict IDH1wt subtype in TCGA (G) and CGGA (H) datasets. (I) Differential expression of *ISG20* mRNA in human normal brain tissues (Normal), human LGG tissues (LGG) and human GBM tissues (GBM). (J) Representative photographs of immunohistochemical staining of *ISG20* in IDH1 mutation status of GBM. (K) Representative photographs of immunohistochemical staining of *ISG20* in human normal brain tissues (Normal), human LGG tissues (LGG) and human GBM tissues (GBM). Positive cells are stained brown. The data are presented as the mean ± SD, $P < 0.05$. * $P<0.05$; ** $P<0.01$; *** $P<0.001$.

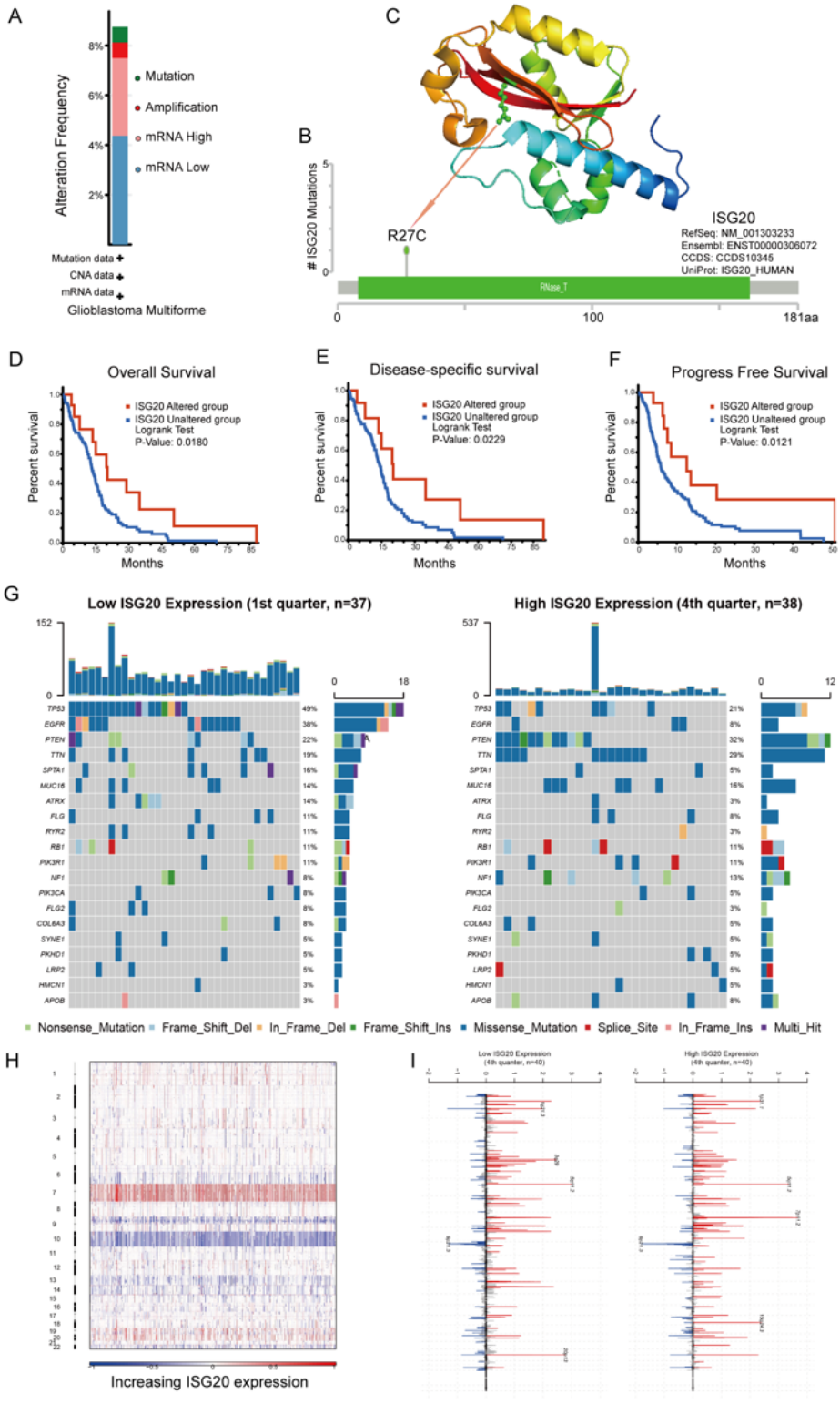

Figure 4

Genetic alteration of *ISG20* in GBM. The alteration frequency with mutation type (A) and mutation site (B) are displayed. We display the mutation site (R27C) in the 3D structure of *ISG20* (C). We also analyzed the potential correlation between genetic alterations and overall survival (D), disease-specific survival (E) and progress-free survival(F) of GBM using the cBioPortal tool. Differential somatic mutations were detected in gliomas with low and high *ISG20* expression (G). The overall CNAs profile in order of increasing *ISG20* expression (H). GISTIC 2.0 amplifications and deletions in gliomas with low and high ISG20 expression (I). Chromosomal locations of peaks of significantly recurring focal amplification (red) and deletions (blue) were presented. $P < 0.05$.

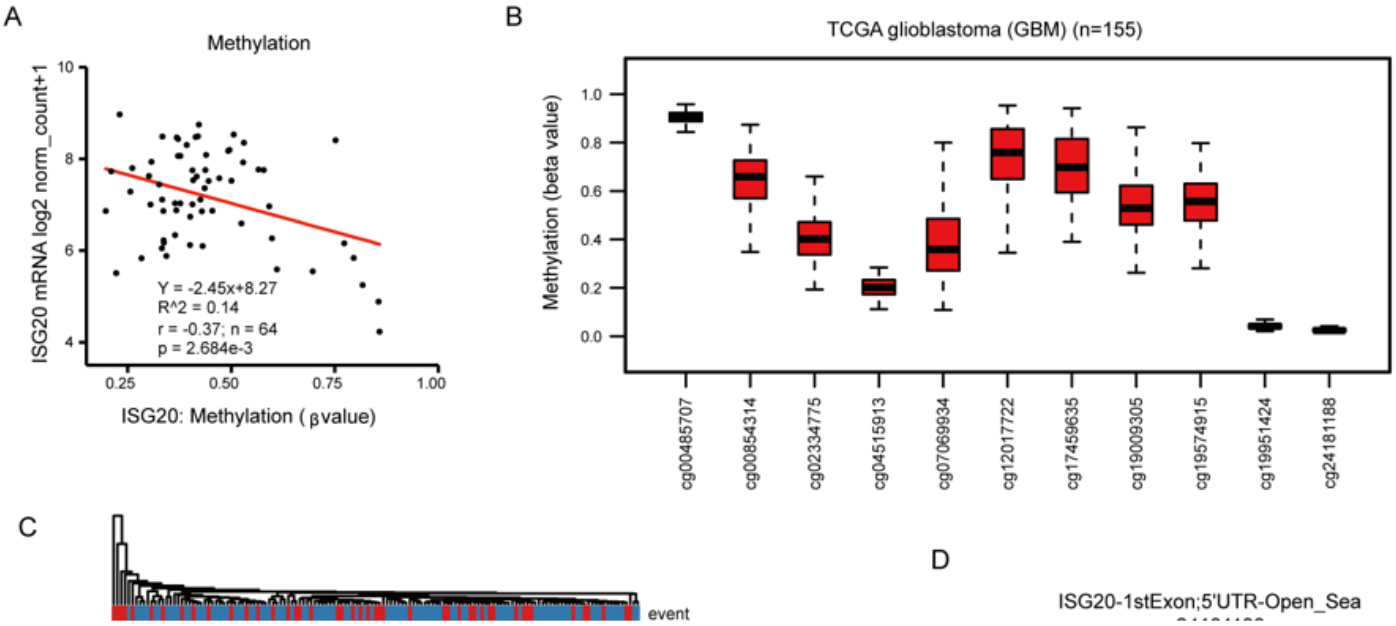

Figure 5

ISG20 DNA methylation and their prognostic values in GBM. (A) The correlation between *ISG20* expression and its DNA methylation was calculated using the cBioPortal online tool for GBM. (B) The beta values of eleven *ISG20* CpG sites in HM450K. (C) The DNA methylation clustered expression of GBM using the MethSurv tool. (D) OS curve of cg24181188 in GBM patients using the MethSurv tool. (E) Linear

correlation scatterplot of *ISG20* CpG sites. *Y*-axis represents mRNA expression fold change (Log10). *X*-axis represents cg24181188 methylation beta value. $P < 0.05$.

Figure 6

Functional Enrichment Analysis of *ISG20* in patients with GBM. (A) 301 genes related ($|R| > 0.5$, $P < 0.05$) with *ISG20* expression were used to draw the heat maps. BP (B), CC (C), MF (D), KEGG(E) and GSEA (F) analysis of the related genes. $P < 0.05$.

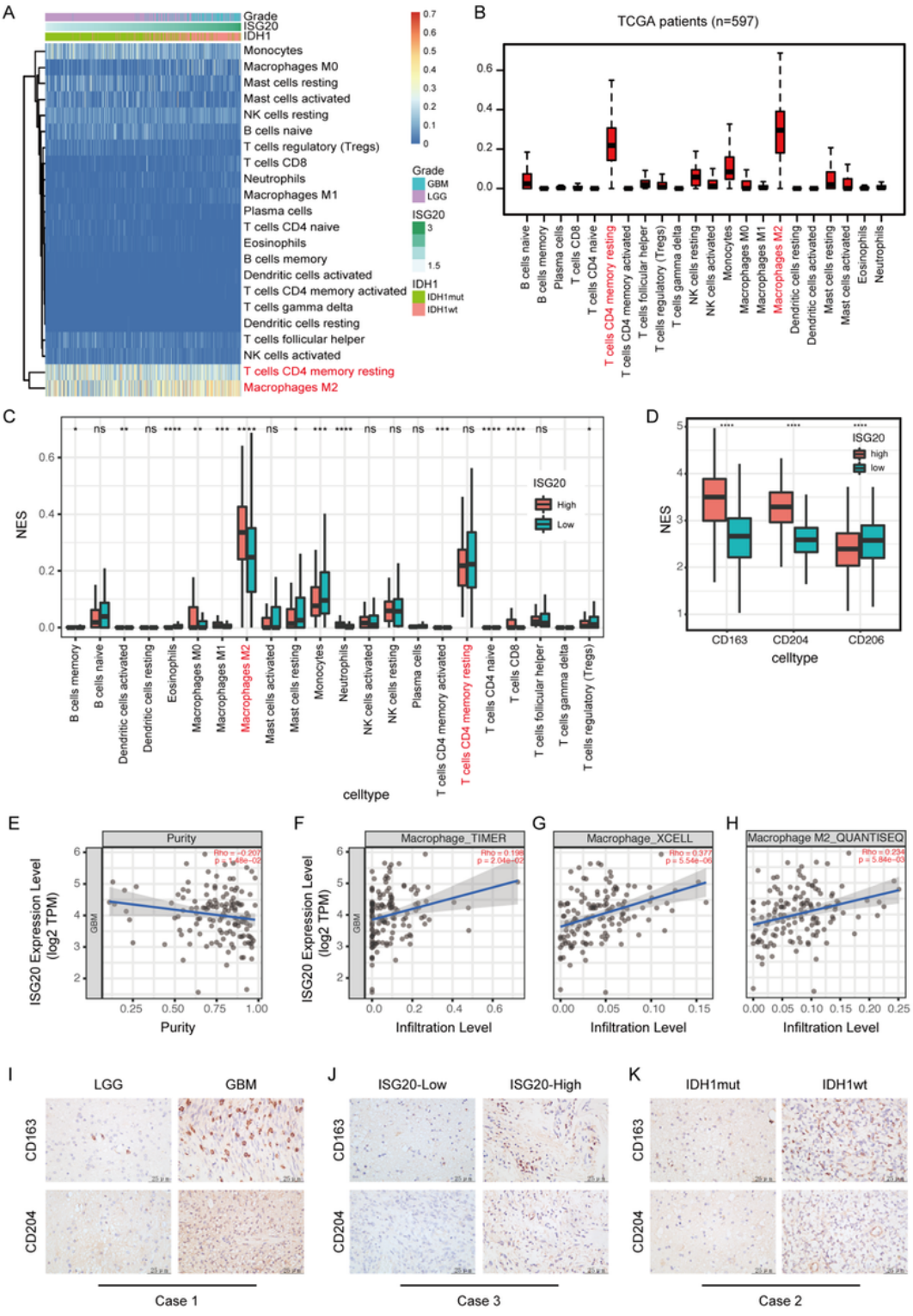

Figure 7

ISG20 expression is associated with immune infiltration levels and macrophages M2 polarization in glioma patients. (A, B) The first two large portion of immune cells were Macrophage M2 and T cells CD4 memory resting. (C) The varied proportions of 22 subtypes of immune cells in high and low *ISG20* expression groups in glioma samples. (D) CD163 and CD204 expression were significantly up- regulated in *ISG20* high expression group. However, CD206 expression was down- regulated in ISG20 high

expression group. (E) The relationship between *ISG20* expression and tumor purity. (F-H) The relationship between *ISG20* expression and Macrophage M2. (H) Representative photographs of immunohistochemical staining of CD163 and CD204 in human LGG tissues (LGG) and human GBM tissues (GBM). (I) Representative photographs of immunohistochemical staining of CD163 and CD204 in *ISG20* high-expression group and *ISG20* low-expression group of GBM. (J) Representative photographs of immunohistochemical staining of CD163 and CD204 in IDH1 mutation status of GBM. Positive cells are stained brown. $P < 0.05$. * $P<0.05$; ** $P<0.01$; *** $P<0.001$; **** $P<0.0001$.

Supplementary Files

This is a list of supplementary files associated with this preprint. Click to download.

- TableS1.docx
- FigureS1.docx
- FigureS2.docx